RESEARCH ARTICLE

STEM CELLS AND REGENERATION

Zebrafish midbrain slow-amplifying progenitors exhibit high levels of transcripts for nucleotide and ribosome biogenesis

Gaëlle Recher[1,2,*], Julia Jouralet[1,3,*], Alessandro Brombin[1,3], Aurélie Heuzé[1,3], Emilie Mugniery[1,3], Jean-Michel Hermel[1,3], Sophie Desnoulez[1,2], Thierry Savy[1,2], Philippe Herbomel[4,5], Franck Bourrat[1,3], Nadine Peyriéras[1,2,§], Françoise Jamen[1,3,6,‡] and Jean-Stéphane Joly[1,3,‡,§]

ABSTRACT

Investigating neural stem cell (NSC) behaviour *in vivo*, which is a major area of research, requires NSC models to be developed. We carried out a multilevel characterisation of the zebrafish embryo peripheral midbrain layer (PML) and identified a unique vertebrate progenitor population. Located dorsally in the transparent embryo midbrain, these large slow-amplifying progenitors (SAPs) are accessible for long-term *in vivo* imaging. They form a neuroepithelial layer adjacent to the optic tectum, which has transitory fast-amplifying progenitors (FAPs) at its margin. The presence of these SAPs and FAPs in separate domains provided the opportunity to data mine the ZFIN expression pattern database for SAP markers, which are co-expressed in the retina. Most of them are involved in nucleotide synthesis, or encode nucleolar and ribosomal proteins. A mutant for the *cad* gene, which is strongly expressed in the PML, reveals severe midbrain defects with massive apoptosis and sustained proliferation. We discuss how fish midbrain and retina progenitors might derive from ancient sister cell types and have specific features that are not shared with other SAPs.

KEY WORDS: Neural stem cell, Optic tectum, Retina

INTRODUCTION

In neural stem cells (NSCs) and neural progenitors (NPs), as in other cell types, cell identity is characterised by specific molecular signatures that depend on the environment provided by neighbouring cells (Fuchs et al., 2004). It is therefore important to study NPs *in vivo*. However, few *in vivo* investigations have been performed so far and these have mainly focused on two telencephalic populations in rodents: the subventricular zone (SVZ) and the dentate gyrus of the hippocampus (Zhao et al., 2008; Chojnacki et al., 2009; Kriegstein and Alvarez-Buylla, 2009; Hsieh, 2012). Teleosts and amphibians display an extraordinary capacity for NP activation and maintenance, but also for self-repair and neuronal regeneration in adulthood (Grandel et al., 2006; Zupanc, 2009; Kizil et al., 2011; Zupanc and Sîrbulescu, 2011; Schmidt et al., 2013). They are therefore excellent models for comparative

studies of the NP-based mechanisms underlying neural regeneration and are suitable for studies involving transgenesis and also for live imaging (Rieger et al., 2011; Rinkwitz et al., 2011).

One of the most interesting neurogenic areas, which has been described in both medaka (Alunni et al., 2010) and zebrafish (Grandel et al., 2006; Ito et al., 2010; Grandel and Brand, 2013), is located at the medial, lateral and caudal margins of the adult optic tectum (OT). The OT is a prominent dorsal region of the midbrain that functions as a cellular 'conveyor belt' (Devès and Bourrat, 2012). In this cortical structure there is a spatiotemporal correlation between the maturation state of a cell and its position in the OT. Each cell population, at a particular level of differentiation, is marked by concentric gene expression patterns. Similarly, the anamniote retina may be considered a cellular conveyor belt and, as discussed in a recent review (Cerveny et al., 2012), tectal cells and retina cells from the ciliary marginal zone (CMZ) share common molecular signatures and express many canonical proliferation markers.

Here we present an integrated study using zebrafish embryos to examine a population of label-retaining multipotent midbrain NPs. This population connects the OT to the torus semicircularis (TS) (a more ventral, but also an alar, midbrain structure) posteriorly and laterally. Medially, it also connects the OT to the cerebellum. Previously described as the 'caudal wall' (Palmgren, 1921) and recently as the 'posterior midbrain lamina' (Grandel et al., 2006), this structure wraps the embryonic OT both posteriorly and laterally; we therefore find it more appropriate to refer to this structure as the 'peripheral midbrain layer' (PML). Three recently published reviews (Cerveny et al., 2012; Grandel and Brand, 2013; Schmidt et al., 2013) pointed out the need to know more about the formation and function of this cell layer, which gives rise to different types of tectal cells. It is in close proximity with the *her5*-positive stem cells (SCs) at the midbrain-hindbrain boundary (MHB) and probably derives from this SC population. However, MHB SC and PML progenitors express different markers (glial and neuroepithelial, respectively) (Chapouton et al., 2006) (reviewed by Schmidt et al., 2013).

The zebrafish is a well-established model system for three-dimensional real-time (3D+time) live imaging of morphogenetic events in the eye and nervous system (England et al., 2006; Greiling et al., 2010; Kwan et al., 2012). However, midbrain development remains poorly studied in this organism. The morphogenetic movements that shape the tectum have not been described. Using two-photon laser-scanning microscopy (TPLSM) for imaging neural tissue, and tracking the behaviour of cells in real time, we provide the first comprehensive analysis of the cellular events that shape the OT. We found that the midbrain is formed in a stepwise manner: intense morphogenetic movements shaping the TS (period 1) are followed by continued elongation of the PML and cytological

[1]CNRS, UPR3294 Unité Neurobiologie et Développement, F-91198 Gif-sur-Yvette, France. [2]MDAM (Multiscale Dynamics in Animal Morphogenesis) group, NED Unit, Institut Fessard, CNRS, F-91198 Gif-sur-Yvette, France. [3]INRA, USC1126, F-91198 Gif-sur-Yvette, France. [4]Institut Pasteur, Macrophages and Development of Immunity, Institut Pasteur, F-75015 Paris, France. [5]CNRS, URA2578, F-75015 Paris, France. [6]Université Paris-Sud, F-91400 Orsay, France.
*These authors contributed equally to this work
‡These authors contributed equally to this work

§Authors for correspondence (peyrieras@inaf.cnrs-gif.fr; joly@inaf.cnrs-gif.fr)

changes without further major morphogenetic movements (period 2). We showed that PML progenitors proliferate slowly by symmetric division. We determined that cells in the PML are slow-amplifying progenitors (SAPs) and turn into fast-amplifying progenitors (FAPs) as they enter into the OT.

Screening expression patterns in the PML allowed us to identify key features of genetic networks that are expressed differentially in progenitors: a network expressed in all proliferating cells (SAP+FAP) and another specific to SAPs. This latter network includes genes involved in ribosome biogenesis and DNA synthesis. We carried out a functional study of the *perplexed* mutant line, which lacks a functional *cad* gene. Our results showed that *cad*, which is strongly expressed only in SAPs, is required more generally for coordinating the cell proliferation and survival of midbrain cells. Therefore, our work leads to the hypothesis that a subset of the ribosome and nucleotide biosynthesis genes, which do not exhibit ubiquitous expression but instead are specific to midbrain SAPs, have a crucial role in proliferating cells during development.

RESULTS

PML morphogenesis occurs in two steps

A histological analysis was carried out on zebrafish embryos from 24 hours post-fertilisation (hpf) to 7 days post-fertilisation (dpf) to study PML morphogenesis. Parasagittal section observations showed that PML can be unambiguously identified in prim-5 stage embryos (24 hpf; end of somitogenesis) (Fig. 1A). At this stage the PML is thick and appears as typical pseudo-stratified neuroepithelium. At 48 hpf (long-pec stage), the PML is a semi-circular layer of cells connecting the OT to more ventral structures originating from the alar neural plate (known as the TS) (Fig. 1C).

There is a similar lateral structure connecting the OT to the TS as seen in transverse sections (not shown). On sagittal sections close to the sagittal plane (Fig. 1D), the medial PML connects the tectum with the medial isthmic proliferation zone, which is itself connected to the cerebellum proliferation zone (CPZ).

The formation of the PML can be divided into two steps: before 48 hpf, the PML undergoes formation as the brain exhibits major morphological changes (period 1); after 48 hpf, the PML structure continues to elongate while the brain grows and the TS and OT become more distant; in addition, PML cells exhibit cytological changes (period 2).

Morphological changes were examined by live imaging of zebrafish embryos expressing nuclear Venus fluorescent protein. Imaging of transverse sections at 26 hpf (during period 1) revealed that, as the tegmentum grows, the TS invaginates and spreads medialwards over the tegmentum from both sides of the embryo (Fig. 1E,F; supplementary material Movie 1). At later stages, proliferation becomes confined to the intermediate zone between the OT and the TS. This lateral proliferation zone becomes marked by slightly more intense staining of the nuclei in the transgenic line. It gradually extends during development and forms the PML between the OT and TS.

We observed no major morphogenetic movements after 48 hpf (period 2); the PML is established and its growth is thereafter coordinated with that of the brain. PML cells undergo prominent cytological changes from a neuroepithelial type (see below) to form a monolayer pavement epithelium. By 7 dpf, these cells are found to be tightly apposed to the posterior side of the OT (Fig. 1A). At this stage, the lateral recesses of the mesencephalic ventricle (located between the tectum and the PML) become invisible (Fig. 1A).
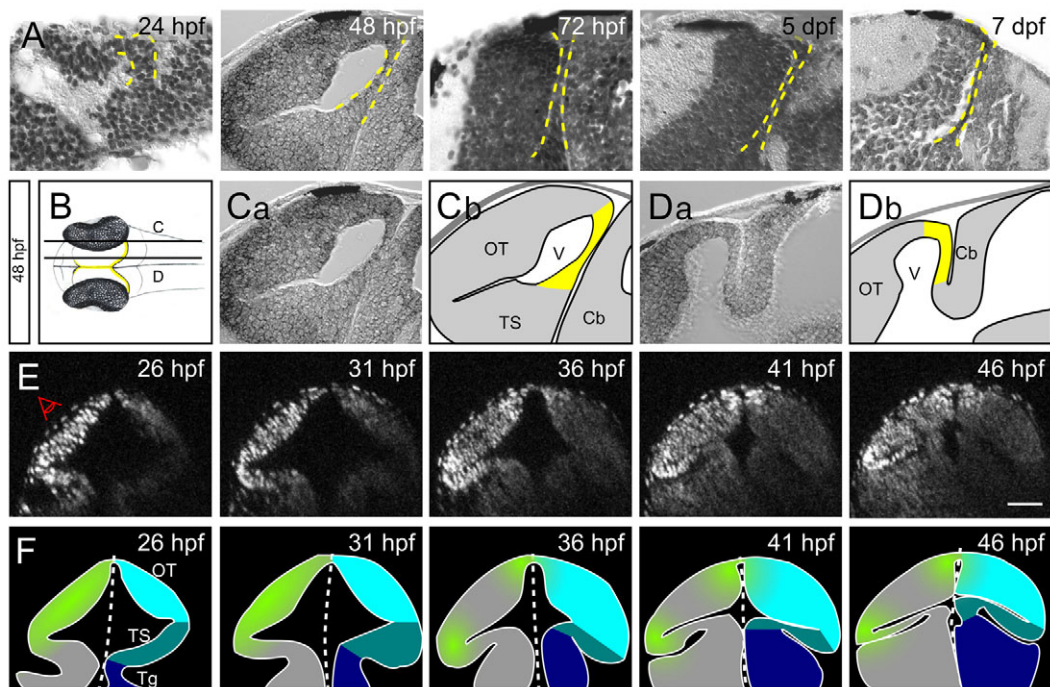

Fig. 1. PML morphogenesis in zebrafish from 1 to 7 dpf. (A) Parasagittal sections of zebrafish from 24 hpf to 7 dpf. As development proceeds, the PML (delineated by a yellow dashed line) becomes thinner and tightly apposed to the OT. (B) Schematic dorsal view of an embryo at 48 hpf. Planes of the sagittal sections in C (more lateral) and D (more medial) are indicated. The PML is found at the margin of the OT (yellow). (C) On lateral sections, the PML connects the OT to the TS. (D) On medial sections, the PML connects the OT to the cerebellum. (E,F) Embryo imaged from its left side (E) and corresponding interpretive schematics (F). Reconstructed midbrain transverse sections were taken at 5-hour intervals. Proliferation (green) becomes restricted to an area between the OT (light blue) and the TS (mid-blue). The tegmentum is in dark blue. Cb, cerebellum; OT, optic tectum; Tg, tegmentum; TS, torus semicircularis; V, ventricle. Scale bar: 50 μm.

PML cells are large polarised neuroepithelial cells that divide in the planar plane

We examined the localisation of two apical markers in PML cells. At 48 hpf, we found that atypical protein kinase C (aPKCζ) and Zona occludens protein 1 (ZO-1), which are markers of adherens and tight junctions, respectively, are expressed on the ventricular side (Fig. 2A). We observed that cells of the PML are polarised and have larger nucleoli (Fig. 2B) than those observed in the OT. The chromatin in PML cells appeared decondensed compared with that in OT cells, as shown by electron microscopy (Fig. 2C). Moreover, PML cells exhibited larger and more elongated nuclei, as observed in live imaging (Fig. 2D).

During mitosis, PML cell nuclei transiently swell (Fig. 2E; yellow cells in supplementary material Movie 2) and migrate to the apical side of the layer to divide [interkinetic nuclear migrations (supplementary material Movie 3) (Baye and Link, 2007)]. This is further evidence of the neuroepithelial nature of the PML, as this movement typically occurs during neuroepithelial-like neurogenesis (Götz and Huttner, 2005). We found that most divisions of PML progenitors are within the plane of the neuroepithelium. Most of the observed mitotic events (94.3%) are planar and only a few (5.7%) are apical-basal (Fig. 2F; supplementary material Movie 2, yellow cells divide in a planar fashion). The mitotic plates rotate and then stabilise in orientation shortly before mitosis to achieve planar divisions (supplementary material Fig. S1); this has been described previously in neuroepithelial cells at earlier stages (Herbomel, 1999; Geldmacher-Voss et al., 2003).

PML cells are SAPs and give rise to FAPs of the OT

To directly examine PML and OT cell cycle lengths, we produced TPLSM 3D+time live imaging datasets of nuclear-labelled transgenic zebrafish (supplementary material Fig. S2). Eight PML nuclei were selected at 30 hpf, digitally tagged with Mov-IT software, and individually tracked (Fig. 3A-C; supplementary material Movie 4). After each mitosis, both daughter cells were followed, resulting in a 15-hour lineage analysis with high spatial and temporal accuracy. We measured an average cell cycle length of 5:51±1:49 hours (*n*=25) in the PML and a much shorter interval between two mitoses of 1:35±1:22 hours (*n*=13) in the OT (Fig. 3G). This shows that, from 30 hpf to 45 hpf, SAPs are located in the PML, whereas FAPs are in the OT. From this lineage analysis we observed that PML cells initially remain in the PML where they divide approximately twice during the whole imaging session (i.e. from 30 hpf to 45 hpf; Fig. 3; an explicit example is given in Fig. 3D-F and in supplementary material Movie 5). Daughter cells are then located around the midbrain ventricle, and at the end of the movie (45 hpf) are seen in the OT (Fig. 3; supplementary material Movies 4, 5). All trajectories are parallel and in the horizontal plane; most of the progeny of any single PML cell remain confined into a small volume in the tectum, such that clonal dispersion is low.

We observed that the progeny of three PML clones contributed to both the OT and the TS [Fig. 3, red (see also supplementary material Movie 6), orange and dark yellow clones].

The PML displays a specific gene expression profile that is shared with the retina CMZ

We looked for potential genetic signatures in PML cells by data mining the ZFIN gene expression database (www.zfin.org/). To distinguish specifically expressed PML genes from those that are more widely expressed in the midbrain (Fig. 4A) we applied several criteria. At the early prim-15 to prim-25 stages (when most tectal cells are still proliferating), expression of a 'thinly' expressed gene
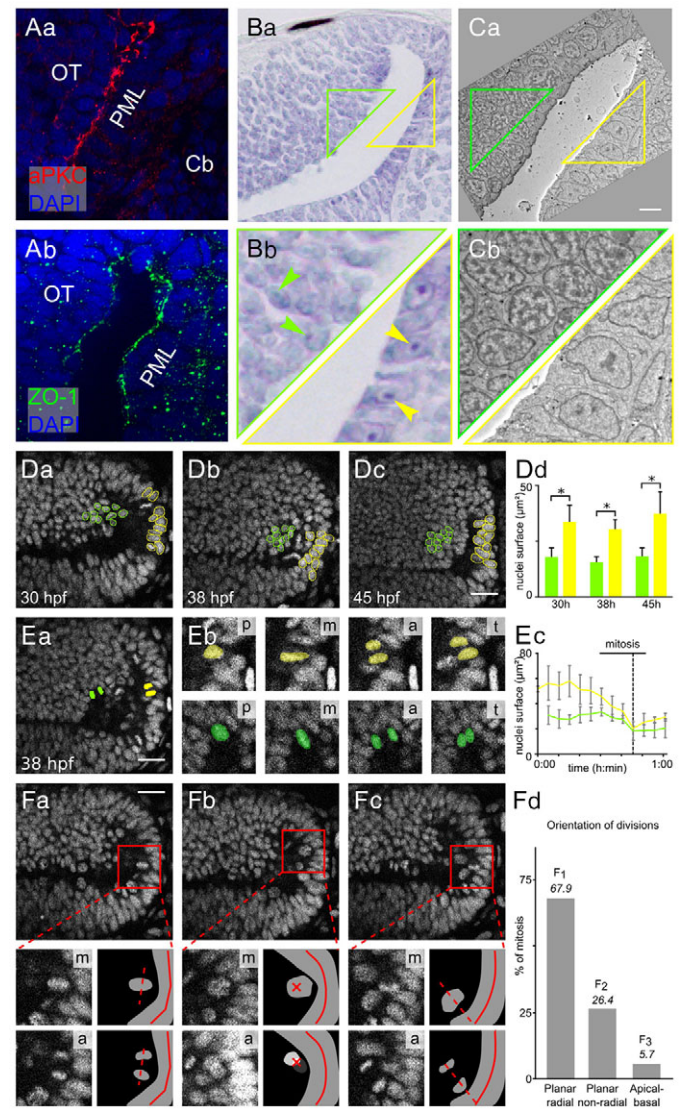

Fig. 2. The PML is a neuroepithelial proliferation zone. (A) Sagittal sections at 48 hpf showing the expression of apical markers in PML cells: aPKC (a) and ZO-1 (b). Nuclei are stained with DAPI. (B) Nissl staining of sagittal sections showing that PML cells (yellow triangle) have larger nuclei with bigger nucleoli than OT cells (green triangle). Arrowheads indicate nucleoli. (C) Electron microscopy image of a sagittal section at 48 hpf showing that PML cells (yellow triangle) have decondensed chromatin, whereas chromatin in OT cells (green triangle) is condensed. (D) Sagittal optical sections of the OT from a *Tg(Xla.Eef1a1:H2B-Venus)* embryo. Interphase nuclei in the PML (yellow) are larger than at the margin of the OT (green). At all stages, the surface areas of the PML and the OT nuclei are significantly different (Mann-Whitney U-test, *P<0.001); error bars indicate s.d. (E) Average PML and OT nucleus size for ten mitoses. (a) Location of tracked nuclei (as detailed in b). p, prophase/prometaphase; m, metaphase; a, anaphase; t, telophase/cytokinesis. (c) M phase is indicated by a dotted line. OT, green; PML, yellow. (F) Mitosis orientations. (a) Planar radial division [30:56 (hours:minutes) hpf]. (b) Planar non-radial division (30:52 hpf). (c) Apicobasal division (31:13 hpf). (Bottom panels) Enlarged metaphase plate (labelled m), subsequent anaphase (labelled a) and corresponding interpretive diagrams. For planar non-radial divisions (b), the two daughter cells are not in the same plane. The anaphase image is the sum of the images centred on the two daughter cells. The red cross indicates the axes of the planar non-radial mitoses. Of 53 mitoses, 36 are planar radial, 14 are planar non-radial and 3 are apicobasal. (d) Non-random predominantly planar radial mitoses according to χ^2 test (*P*<0.001). Cb, cerebellum; OT, optic tectum; PML, peripheral midbrain layer. Scale bars: 20 μm.
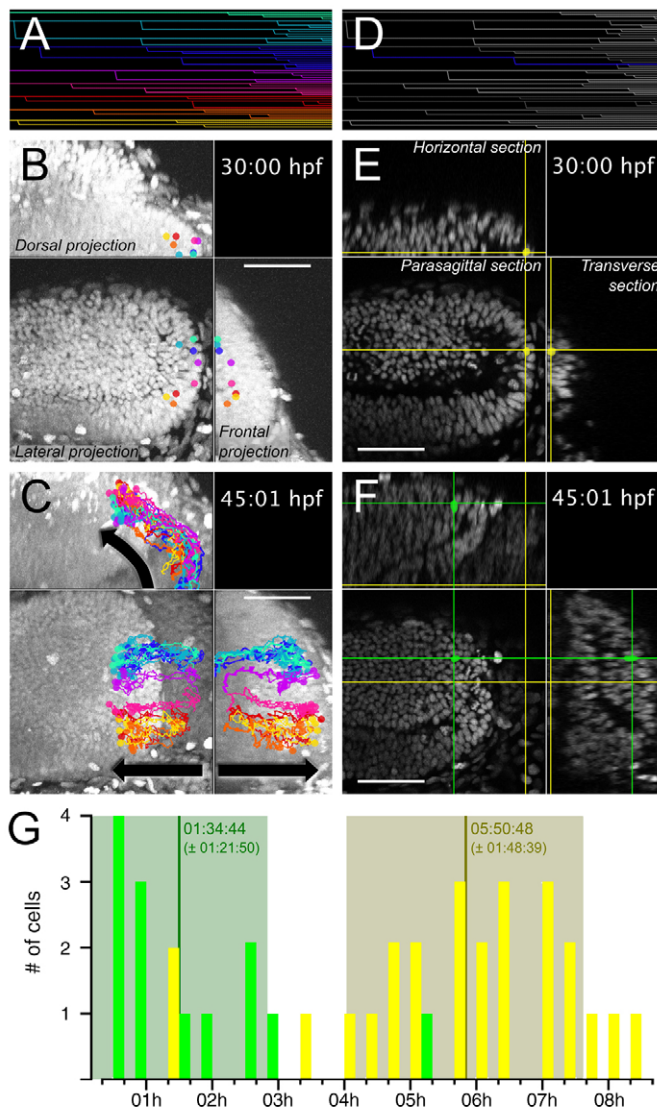
Fig. 3. Slow-amplifying PML cells give rise to tectal FAPs. PML cells were tracked from 30:00 hpf to 45:01 hpf. The complete lineage tree is shown in A. Cells originating from the PML at 30 hpf are found in the external part of the OT 15 hours later (B,C). In B and C, eight clonal cell trajectories, as indicated with different colours, have been overlaid on a volume projection of the left midbrain. The dots indicate the position of the cells at 30 hpf (B) and 45:01 hpf (C) and the lines trace the past trajectory of each clone. For the full movie, see supplementary material Movie 4. (D-F) A clone (represented by the intersection of the cross at the corresponding sagittal, horizontal and transverse planes) is followed from the PML, where it achieved two mitoses (E), to the OT, where two further mitoses occurred (F). For the full movie, see supplementary material Movie 5. (G) Cell cycle durations are separated into two clusters: OT (green) FAP cycles, 1:35±1:22 hours (n=13); PML (yellow) SAP cycles, 5:51±1:49 hours (n=25). Scale bars: 50 µm.

had to be restricted to the peripheral part of the midbrain and not be ubiquitously expressed throughout the whole proliferating midbrain (in the way that proliferation-associated markers are at that stage). At later stages (high-pec to long-pec) the midbrain expression domain had to be thin and restricted to the PML in Nomarski images. Since a striking synexpression in tectum and retina was observed (see below), we also used another criterion: the identification of a ring of retina cells tightly surrounding the lens. More widely expressed genes, associated with all progenitors, are expressed in a wider ring corresponding to proliferative cells of the

CMZ (supplementary material Fig. S3). We found 117 genes associated with proliferation (supplementary material Fig. S3, Table S1). Of these, 68 genes are expressed in a relatively large region of the peripheral OT and of the CMZ, whereas 49 display a very thin expression pattern located at the most peripheral part of the OT and in the most central part of the CMZ (supplementary material Fig. S3). We also added a further two genes to this second category: *ect2* and *nop56* (*nol5a*) (supplementary material Table S1). These were identified from a previous *in situ* hybridisation screening performed on medaka (data not shown) and their specific expression was also confirmed in zebrafish (Fig. 4Ae,f,Cb,c). ZFIN data mining results are presented in supplementary material Fig. S3.

We carried out whole-mount *in situ* hybridisation (WMISH) and histological analysis on a subset of proliferation-associated genes to confirm the data mining results. We identified a group of genes, which included *pcna*, with expression that encompasses both FAPs and SAPs (Fig. 4Aa-c). Other genes, such as *nop56*, display a tight expression pattern that is restricted to PML SAPs (Fig. 4Ad-f). We carefully checked that these PML-associated patterns correlate with expression in SAPs. We found that transcripts of the *pescadillo* (*pes*) gene specifically localise in neuroepithelial cells with large oval nuclei – cells that we called SAPs (Fig. 4B). We also performed WMISH for four genes (*cad*, *ect2*, *nop56* and *pes*; see Fig. 4C) with a very long incubation time (several days) in the staining solution to demonstrate that PML gene expression patterns are really restricted to SAPs.

Two main gene categories are overrepresented in the PML-specific dataset

To define groups of genes with similar functions, we performed several *in silico* analyses. Gene Ontology (GO) term analyses show that, in both of our lists, genes regulating specific cellular functions are overrepresented (Fig. 5; supplementary material Fig. S4). Most genes associated with the proliferation zones of the OT and the PML encode components of the nucleus linked to the global proliferation machinery, more specifically to the machinery regulating cell cycle phases or DNA replication (supplementary material Fig. S4). By contrast, the PML dataset contains mainly genes encoding either nuclear proteins that are active in nucleotide synthesis or nucleolar proteins (Fig. 5A,B). An interaction network analysis using Ingenuity software identified several clusters of PML-specific genes (Fig. 5C), one of which corresponds to a subset of genes encoding proteins involved in rRNA processing (such as *nop56*, *nop58*, *fibrillarin*, *pes*, *wdr12* and *nle1*) (Fig. 5C; supplementary material Table S1).

Interestingly, gene networks already identified by a functional RNAi screen as crucial for *Drosophila* neuroblasts are very similar to the PML progenitor-specific networks (supplementary material Fig. S4) (Neumüller et al., 2011). To test the relevance of our dataset with other SC sets, we compared the identified genes with previously assembled mammalian datasets by searching the Molecular Signature Database MSigDB (v3.0) (Subramanian et al., 2005). Our set of PML-specific genes is enriched for genes that are represented in different cancer-associated gene sets (supplementary material Table S2) and, more importantly, in the PluriNet network (Müller et al., 2008) related to human pluripotent stem cells. This study (Müller et al., 2008) indicates that pluripotent cells exhibit a small number of generic molecular signatures, the functions of which are often linked to the maintenance of pluripotency.

The proliferation and survival of tectal progenitors are affected in the *perplexed* mutant

Many genes considered as housekeeping genes exhibit preferential expression in the PML. To test whether these genes play specific
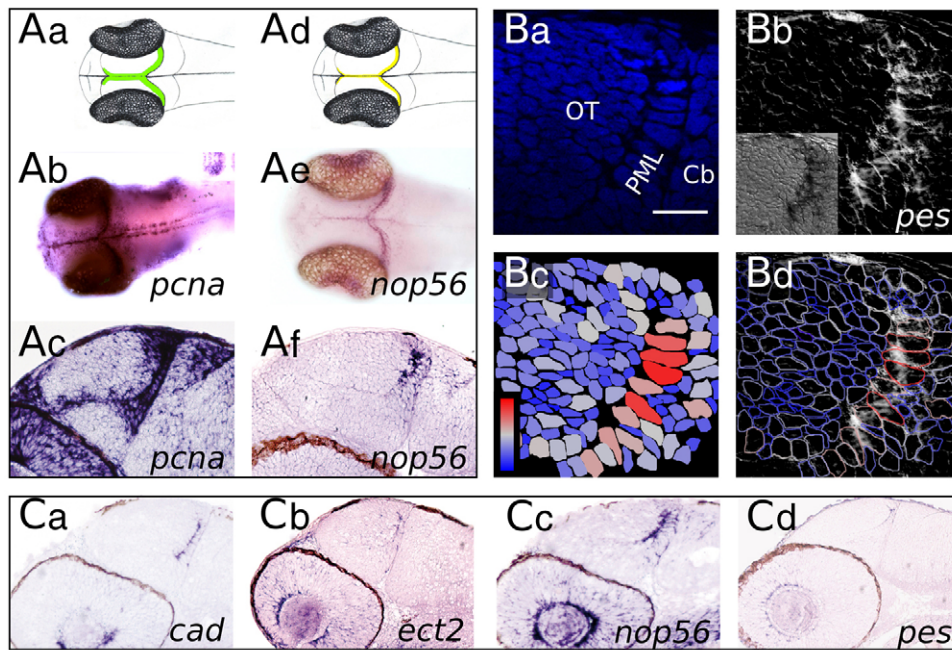
Fig. 4. Transcript distribution in the midbrain: 'large' and 'thin' domains. (A) Whole-mount embryos (b,e) and parasagittal sections (c,f) following *in situ* hybridisation (ISH) with *pcna* (b,c) and *nop56* (e,f) probes. *pcna* is expressed in a 'large' domain containing all proliferating cells. The *nop56* expression domain is 'thin' and restricted to PML SAPs. (B) The *pes* ISH signal colocalises with PML cells (the largest midbrain cells). (a) Nuclear DAPI staining. (b) Inverted colour brightfield image of the same field showing the *pes* ISH signal. Inset shows the real colour brightfield image. (c) Colour-coded nuclei surface. On the blue-red scale, red corresponds to 22 µm² and dark blue to 0 µm². (d) Overlay of the inverted brightfield image with the nuclei border colour-coded drawing. Red nuclei exhibit a strong *pes* ISH signal. (C) Sagittal sections of embryos at 2 dpf. ISH long staining time emphasizes PML-specific gene expression. Scale bar: 10 µm.

roles in PML progenitors, we performed an analysis of the *perplexed* mutant, which lacks a functional *cad* (*carbamoyl-phosphate synthetase 2, aspartate transcarbamylase, and dihydroorotase*) gene, which encodes three enzymes involved in *de novo* pyrimidine biosynthesis (Willer et al., 2005). At 48 hpf, we observed that the PML and OT remain recognisable in *perplexed* mutants but their morphologies are strongly affected. The PML appears thicker than in wild-type embryos (Fig. 6A,B). Throughout the midbrain region, the density of cells is low and there are numerous acellular holes. We imaged midbrains of *perplexed* mutants by TPLSM, but apoptosis rates were so high that we were not able to track cells for an entire cell cycle (data not shown). Massive cell death was detected in mutant OT after TUNEL staining (Fig. 6C,D). We monitored proliferation levels by phospho-histone H3 (pH3) immunostaining at 48 hpf. M-phase cells are present in the proliferative areas (FAP areas) of the tectum and of the TS in *perplexed* mutants (Fig. 6E,F). However, more M-phase cells are visible in the central part of the OT in mutants than in wild types. This was confirmed by Pcna immunostaining at later stages (72 and 96 hpf), when proliferation zones become narrower. In wild type, Pcna expression is restricted to the margin of the OT (FAPs) and PML (SAPs), whereas in *perplexed* mutants Pcna-positive cells are found throughout the whole OT and cerebellum (Fig. 6G-J).

DISCUSSION
The PML is formed of neuroepithelial SAPs that give rise to both OT and TS
We have shown in this study that PML cells exhibit the prototypical features of neuroepithelial progenitors. Located in the largest structure of the fish brain (the OT), PML cells are particularly suitable for studies of the functional and structural characteristics of NPs. We provide an extended description of PML progenitors and highlight how the teleost PML can be used as a model for the characterisation of molecular pathways acting in neuroepithelial SAPs.

The large majority of cell divisions occurring in the PML are planar divisions, although we observed a few apicobasal divisions. In the zebrafish telencephalon, radial glial cells predominantly undergo symmetric gliogenic divisions, which amplify the NSC pool (Rothenaigner et al., 2011). The reason why fish seem to preferentially use this growth mode remains unknown, but it has been shown that a planar orientation of mitoses in neuroepithelia is required for the maintenance of layered structures (Peyre et al., 2011).

We demonstrated that the cell cycle takes about four times longer in the PML than in the OT. To understand the biology of these SAPs, it will be important to identify the factors that induce this relative quiescence in PML cells (see below).

Cells exhibit a major cytological transition when they enter the tectum: from a neuroepithelial phenotype, establishing contacts with the ventricle (apically) and with the pial/basal membrane, to small round cells that sometimes lack contacts with either the pial/basal membrane or the ventricle (data not shown). This transition is apparently correlated with a substantial shift in proliferation rates. It will be interesting to study the factors, positions or cell contacts that trigger this major phenotypic transition. Several well-known signalling molecules are known to induce a fast proliferation mode. For example, sonic hedgehog (Shh) may have a prominent role in the acceleration of cell divisions, as it does in the retina (Locker et al., 2006). The control of progenitor proliferation in the tectum has been shown to be substantially affected in several mutants of the hedgehog pathway (Koudijs et al., 2005).

Our results confirm on live specimens that the OT is a typical cellular conveyor belt (Devès and Bourrat, 2012); it has zones of unmixed FAPs and SAPs at its periphery, a zone of cells exiting the cycle and a central zone of differentiating cells (Cerveny et al., 2012) (Fig. 7). Our data show centripetal movements of the progenitors when they enter the tectum. However, we believe that these movements are not due to active migration but rather to passive displacements resulting from intensive cell division. It would be interesting to analyse more globally the major directions of cell displacements that shape the OT, PML and TS (using automated cell tracking and visualisation of kinematic descriptor maps).

None of the tracked cells remains in the PML to replenish the SAPs. One hypothesis is that the bona fide SCs of the PML are localised more medially in the isthmic proliferation zone and
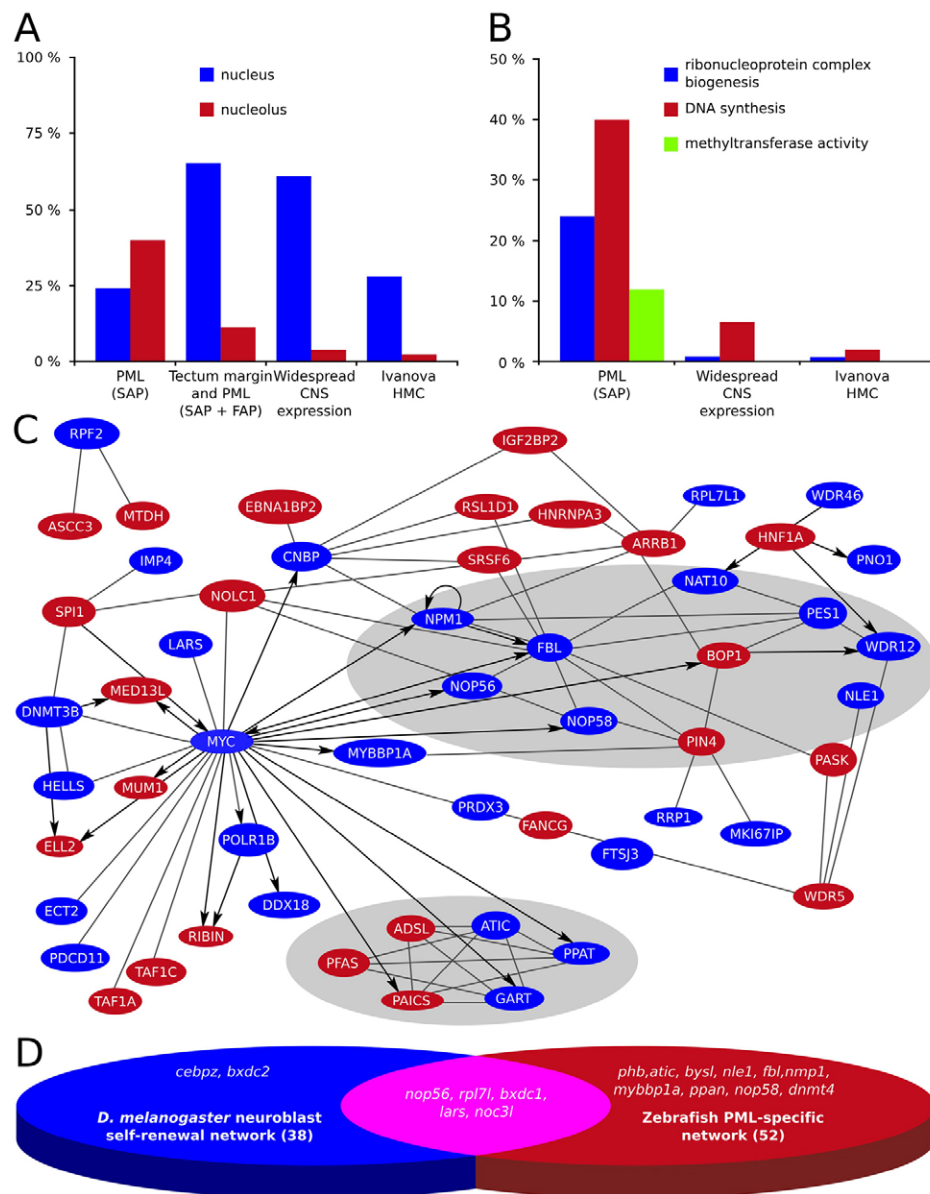
Fig. 5. The PML gene network contains genes encoding nucleotide biosynthesis enzymes, nucleolar components and ribosomal proteins. (A,B) Gene ontology (GO) enrichment analysis of the PML-specific gene list, using the CNS and Ivanova hematopoiesis mature cells (HMC) gene lists as backgrounds. (A) Cellular localisation: genes encoding nucleolar proteins are overrepresented in the PML dataset. (B) Cellular function: in the PML dataset, genes involved in ribosome biogenesis and nucleotide synthesis are overrepresented. (C) Ingenuity pathway analysis of the main gene network for the PML dataset. Two distinct molecular clusters are outlined (grey): nuclear proteins mainly involve purine biosynthesis, and nucleolar proteins involve rRNA and ribosomal processing. PML genes are in blue and genes not included in our study are in red. Arrows starting from *myc* indicate direct Myc target genes or partners. (D) Overlap between fish and *Drosophila* NSC lists.

correspond to the *her5*-positive population described by Chapouton et al. (Chapouton et al., 2006).

We found that the PML contains a subset of progenitors that gives rise to both the OT and TS. It is striking that a single progenitor is able to generate cells belonging to two distinct brain structures. This unusual and unexpected dual contribution seems to be dependent on the location of the tracked progenitor in the PML with respect to the dorsoventral axis. This feature was already proposed by Grandel et al. (Grandel et al., 2006), who noted that the TS has no specific zone of progenitors. However, their study was performed on adults and did not provide any evidence for the location of early TS progenitors. In the mouse embryo, some progenitors have the capacity to populate more than one neural structure; for example, the diencephalon and telencephalon (Mathis and Nicolas, 2006).

PML cells express genes active in stem cells and tumour cells

Pluripotent embryonic SCs have the widest possible capability for gene transcription. As they become more specialised, they refine their transcriptional repertoire (Efroni et al., 2008). In our model of pluripotent neural cells (the SAP/PML cells), we identified different groups of genes as described below according to the function they fulfil.

One PML cell-specific group contains genes known to play major functions in SCs and tumour cells, where they either contribute to the regulation of DNA methylation (*dnmt4* and *hells*) (Law and Jacobsen, 2010) or inhibit cell apoptosis (*ppan*) (Bugner et al., 2011).

PML cells also express *bystin* transcripts that have been reported to be expressed in type B SCs and in lesioned rat cerebral cortex (Sheng et al., 2004).

Prohibitin (Phb), which is often associated with cancer, is an inhibitor of cell proliferation (Mishra et al., 2006) that could potentially trigger the slowing of progenitor cell divisions. Indeed, genes known to promote definitive cell cycle exit in the differentiating cells of the OT [such as cyclin-dependant kinase inhibitors, *gadd45* or *insm1* (Candal et al., 2004; Candal et al., 2007)] were found not to be expressed in PML progenitors (data not shown). This suggests that the mechanisms inducing quiescence in SCs are distinct from those promoting cell cycle exit during terminal differentiation.
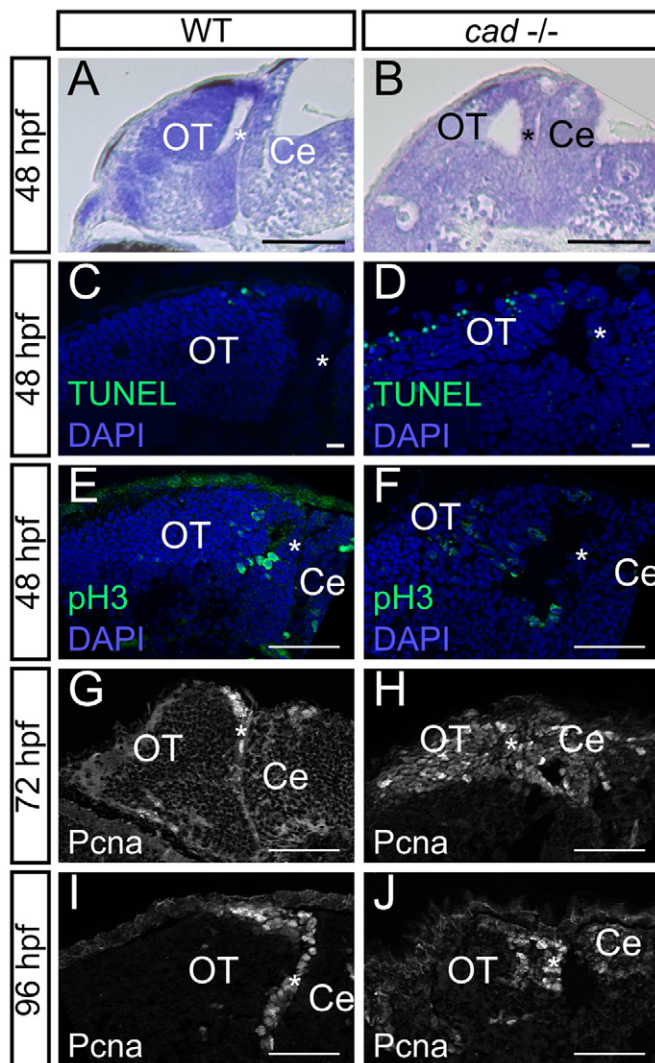
Fig. 6. Absence of *cad* function in homozygous mutant embryos leads to proliferation defects and massive cell death in the midbrain.
(A,B) Sagittal sections of wild-type (A) and *perplexed* (B) embryos with Nissl staining at 48 hpf. *perplexed* mutant displays atrophy of the tectum and PML thickening. (C,D) Sagittal sections following TUNEL staining at 48 hpf. More apoptotic cells are observed in *cad⁻/⁻* (D) than in wild-type (C) embryos. (E,F) Phospho-histone H3 labelling at 48 hpf showing the presence of proliferative cells not only in the periphery of the tectum but also in the central part in *perplexed* mutants. (G-J) Pcna immunostaining at 72 and 96 hpf showing persistence of wide proliferation zones in the OT of *perplexed* mutants at late larva stages. Anterior is at the left and dorsal at the top of each image. OT, optic tectum, Ce, cerebellum. The asterisk indicates the PML. Scale bars: 100 µm in A,B; 10 µm in C,D; 20 µm in G; 50 µm in E,F,H-J.

Among the PML cell-specific gene network we identified *c-myc* (*myca* in zebrafish), which is known to be a master regulator of normal cell growth and proliferation (Liu et al., 2008) (Fig. 5D; supplementary material Fig. S3Y2,4) and could play a specific role in SAPs. In *Xenopus*, *c-myc⁺/n-myc⁻* cells were shown to be candidates for a restricted population of retinal SCs found in a subdomain at the tip of the CMZ (Xue and Harris, 2011). Transcripts of several Myc targets are also restricted to the PML (see below; Fig. 5). The gene *mybbp1a* is located at a key node of the established PML network. This gene has been shown to activate *p53* when ribosome biogenesis is suppressed (Tsuchiya et al., 2011) and Mybbp1a might be part of a nucleolar pool of proteins involved in mitotic progression (Perrera et
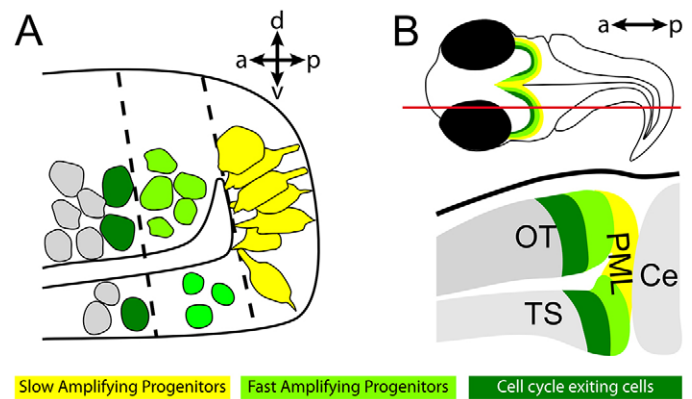

Fig. 7. The PML contributes to the formation of the OT and of the TS.
(A) At the periphery of the OT, there are two types of neural progenitors. PML cells (yellow) are SAPs and have big nuclei and contact both apical and basal with membrane extensions. They turn into SAPs (light green) with smaller nuclei when they enter the OT or the TS, then they exit the cell cycle (dark green) and differentiate. (B) Top panel: the previously described differentiation gradient forms a concentric gradation when viewed in horizontal section and correlates with observed gene expression patterns. Red line indicates the parasagittal section shown in the bottom panel. OT, optic tectum; TS, torus semicircularis; Ce, cerebellum; PML, peripheral midbrain layer.

al., 2010). Further studies are needed to clarify the role of Mybbp1a in NSCs and SAPs by focusing on the interplay between its nucleolar and cell cycle-associated functions.

Other genes found to be specifically expressed in the PML encode nucleotide biosynthesis enzymes, nucleolar components and ribosomal proteins.

A large PML-specific gene network encodes nucleolar proteins

Genes encoding nucleolar proteins are present in the PML network. Cancer studies have proposed putative instructive roles for nucleolar proteins in tumorigenesis, highlighting their potential role in the control of cell proliferation (reviewed by Ruggero and Pandolfi, 2003). PML nucleolar genes encode proteins belonging to two main complexes. Nop56, Nop58 and Fibrillarin are small nucleolar ribonucleoproteins (SnoRNPs) that are associated in a complex involved in the processing and modification of rRNA. Transcripts encoding Nop56/58 are signatures of fish PML progenitors (this study), but also of the fish (Fig. 5) and *Xenopus* (Parain et al., 2011) retina. The Wdr12, Pes and Bop1 proteins are associated with PeBoW, a complex crucial for the maturation of the large ribosomal subunits in mammalian cells (Hölzel et al., 2005). *pes* was first identified in zebrafish for promoting proliferation in the CNS (Allende et al., 1996). *nle1* and *wdr12* are involved in the biogenesis of ribosomal pre-60S particles. Interestingly, *nle1* is also required for the maintenance of adult hematopoietic stem cells (HSCs) in mice, as shown by conditional knockouts (Le Boutellier et al., 2013).

The expression of genes coding for ribosomal protein is crucial in SCs and SAPs

Ribosomal genes are thought to be ubiquitously expressed and to have strong and early deleterious effects. It is therefore surprising to observe that PML genes encoding ribosomal proteins have restricted transcription patterns and that some have a mild mutant phenotype. For example, zebrafish *rpl7l1* is specifically expressed in PML and CMZ progenitors (supplementary material Fig. S4) and the *rpl7l1* mutant apparently has a mild phenotype (source: ZIRC). By contrast,

its paralogue *rpl7* has been demonstrated to be strongly and ubiquitously expressed (Bradford et al., 2011). A similar situation might occur in *Drosophila*, where *RpL7* has been shown to be specifically required in neuroblasts to maintain their proliferation (Neumüller et al., 2011), whereas its counterpart (*RpL7-like*) displays ubiquitous expression. Another zebrafish study shows that *rpl22l1* and *rpl22* play essential, distinct and antagonistic roles in HSCs (Zhang et al., 2013). Since protein synthesis does not seem to be affected in mutants, these two genes might have some extra-ribosomal functions in the regulation of HSCs. Proteins regulating ribosome synthesis seem to be essential for germline stem cell (GSC) maintenance and function in the gonads of *Drosophila* (Fichelson et al., 2009). The accumulation of specific ribosomal proteins in PML cells creates a signature that distinguishes SAPs from FAPs and other cells of the OT. Recent discoveries of ribosome codes in yeast (Komili et al., 2007) and vertebrates (Kondrashov et al., 2011) highlight the importance of such gene expression signatures.

A PML gene network encodes nucleotide biosynthesis enzymes

One PML cluster contains genes involved in pathways of purine synthesis (such as *gart*, *ppat*, *atic*), pyrimidine biosynthesis [such as *cad* (see also below) and *ctps1a*] and nucleotide metabolism (such as *shmt2*, which has been shown to be regulated by *myc*) (Fig. 5; supplementary material Table S1). It is surprising that transcripts encoding nucleotide biosynthesis proteins accumulate only in SAPs and not in all proliferating cells. In cell culture, *cad* activity is strongly upregulated when cells enter the proliferative phase, and then dramatically downregulated as the culture becomes confluent (Sigoillot et al., 2002).

Are PML cells storage chambers?

We chose to analyse the *perplexed* mutant, which lacks a functional *cad* gene, because a previous study carried out in the retina had already highlighted the importance of this gene for NP proliferation and differentiation (Willer et al., 2005). *perplexed* mutants exhibit no lamination of the retina (Link et al., 2001; Willer et al., 2005). Similarly, we observed that they lack a laminated tectum. The presence of a large number of Pcna-positive cells all over the OT indicates that the cell cycle is dysregulated in midbrain progenitors. In time-lapse analysis, cell cycle intervals could not be precisely measured owing to massive apoptosis in mutant OT. Hence, our hypothesis is that, in *perplexed* mutants, because of the absence of *de novo* nucleoside synthesis, tectal cells, as with retinal cells (Willer et al., 2005), do not undergo proper mitoses and remain blocked in M phase and eventually undergo apoptosis. Indeed, in the eye it has been shown that retinoblasts with the *perplexed* mutation require twice as long to complete one cell cycle (Willer et al., 2005). It is known that the *de novo* pathway of pyrimidine synthesis is most active during growth and development, after which the salvage pathway predominates (Anderson and Parkinson, 1997). Since metabolic intermediates along this pathway do not accumulate, the level of uridine monophosphate (UMP) production relies on Cad activity. Thus, we propose that neuroepithelial cells accumulate high levels of Cad enzymes so that OT FAPs can subsequently perform their rapid divisions without *de novo* synthesis of nucleotides. More generally, the accumulation of machineries composed of many different nucleolar/ribosomal proteins or nuclear proteins might point to key roles for these proteins in the biology of these slowly dividing cells, which have high transcriptional and translational activity (Efroni et al., 2008). We speculate that PML cells, which are poised for subsequent rapid divisions, serve as 'storage chambers'

and thus allow the FAPs to bypass *de novo* synthesis during their intense proliferative activity. This would be similar to the early development strategy whereby maternal components are stored in the huge pluripotent egg cell in readiness for subsequent rapid divisions of the blastomeres.

PML genes are also expressed in the CMZ: evidence of deep homology?

Other PML genes could also have a prominent function in the fish midbrain and eye. Cytological and molecular signatures may help to define cell type homologies from an 'evo-devo' perspective (Arendt, 2005). Synexpression of genes in retinal CMZ cells and midbrain progenitors has been noted (Cerveny et al., 2012; Ramialison et al., 2012) and the phenotypes of mutants for at least 18 PML-specific genes are illustrated on the ZIRC website (supplementary material Table S3). These mutants share strikingly similar neuroectodermal and ocular defects. Heads and eyes appear smaller and necrosis is often reported in the CNS. Further analyses of these mutants are needed to confirm whether these PML genes affect the midbrain neuroepithelial progenitors, in the way that *cad* does.

At early stages of development, more than one-third of the PML-specific genes (according to the ZFIN database) are expressed in the anterior brain region located between the zona limitans intrathalamica and the MHB. This area is proposed to have derived from that of an ancient bilaterian ancestor (Steinmetz et al., 2011). From an initial situation in urbilateria in which rows of lateral (so-called intermediate) progenitors would have participated in both alar forebrain and midbrain morphogenesis, extent vertebrates now evaginate optic cups and their progenitor zone, called the CMZ, whereas the midbrain progenitors in the PML invaginate as revealed in this study. We therefore suggest that retina and midbrain progenitors might be 'sister' cell types with a common evolutionary origin.

Conclusions

We have characterised a population of neuroepithelial midbrain progenitors in zebrafish embryos. Their specific features (long cell cycles, distinctive genetic signatures) emphasize the diversity of NPs in vertebrates. Our work highlights that the PML provides a very useful model with which to study NPs and NSCs. Indeed, we propose that these progenitors have specific metabolic activities and use specific ribosome biogenesis pathways. Future studies should also reinforce interest in this cell type by stressing its role in regenerative processes or in modified nutritional contexts.

MATERIALS AND METHODS
Fish
Zebrafish (*Danio rerio*) wild-type strains (AB and TU) and *perplexed* mutants (*cad^{a52}*) (ZIRC, Eugene, OR, USA) were reared and staged as previously described (Kimmel et al., 1995). For wild-type live imaging, we used a transgenic fish line *Tg(Xla.Eef1a1:H2B-Venus)* to track nuclei. Additionally, we used a double-transgenic fish line resulting from a cross between *Tg(Xla.Eef1a1:H2B-mCherry)* (gift from Georges Lutfalla, Université Montpellier 2, Montpellier, France) and *Tg(Xla.Eef1a1:EGFP-Hsa.HRAS)*.

Two-photon live imaging
To avoid pigmentation zebrafish embryos were treated with 1-phenyl 2-thiourea (0.003%; Sigma), anaesthetised with tricaine (170 μg/ml; Sigma), dechorionated, mounted in 1% standard agarose moulds and covered with 0.5% low melting point agarose. Embryos were imaged laterally and imaging field was focused on the left midbrain. Non-invasiveness was assessed by comparing mitosis between TPLSM and Nomarski imaging (supplementary material Fig. S1). Live imaging was performed using

custom-made two-photon microscopes (BioEmergences). The set-ups are based on a DM6000 and a DM5000 upright microscope (Leica) with 980 nm (Mai Tai, Spectra-Physics/Newport Corporation) and 1030 nm (t-Pulse, Amplitude Systems) excitation wavelengths. Other settings/parameters: objectives, Leica 1.0 NA 20× W (HCX APO) or Olympus 0.95 NA 20× W (XLUMPlanFluo); filters, 525/50 nm (Venus and EGFP), 610/75 nm or 595/45 nm (mCherry); scan speed, 700 Hz; frame average, 3; 512×512 pixels at 0.3 or 0.4 μm wide; a full z-stack was compiled in ~5 minutes. To check that imaging was not deleterious, larvae were allowed to recover in tricaine-free embryo medium until able to feed.

3D+time image analysis

After acquisition, raw images were converted into VTK format and processed with Fiji for rendering and other analysis. We also used the Mov-IT software developed by BioEmergences (Olivier et al., 2010), which enables smooth navigation in orthoslices or in volume rendering acquired at different times, fate map visualisation, and the export of lineage trees with all quantitative information related to cellular dynamics.

Electron microscopy

Zebrafish embryos were anaesthetised at 48 hpf in tricaine (170 μg/ml; Sigma) and rapidly prefixed in fixative A (2.5% paraformaldehyde and 2.5% glutaraldehyde in 0.1 M sodium cacodylate buffer pH 7.2). Embryo heads were dissected and prefixed in fixative A for 12-18 hours at 4°C and then embedded in 1% low melting point agarose and oriented in agarose cubes (<1 mm^3). Heads were kept at 4°C and prefixed for a further 12-18 hours. After infiltration in Epon 812 (Electron Microscopy Sciences), blocks were oriented in moulds and left to polymerise for 48 hours at 60°C. Sections (50-60 nm) were cut using a Leica EM UC6 ultramicrotome and a Diatome Histo-Jumbo diamond knife. After intensification in uranyl acetate and lead citrate, the sections were observed using a JEOL 1400 electron microscope (120 kV) and pictures were taken using a SC1000 Orius GATAN camera.

Histology

Whole-mount in situ hybridisation (WMISH) was performed as previously described (Xu et al., 1994). Antisense riboprobes and paraffin sections were prepared as previously described (Brombin et al., 2011). Sequences of the DIG riboprobes used for in situ hybridisation are given in supplementary material Table S4. Brightfield imaging was performed with a Leica DMRD microscope (Nikon Eclipse E800 camera) or a Nikon AZ100 microscope (Nikon Digital Sight DSRi1). For cryosections, embryos were first protected by incubation in 30% sucrose in phosphate-buffered saline (PBS) for 12-16 hours at 4°C, then embedded in OCT Compound (Sakura), stored at −80°C, and sectioned at 14 μm using a Leica cryostat. Antisera were rabbit anti-phospho-H3 (1:1000; CR10, Millipore), rabbit anti-aPKCζ (1:200; C-20, sc-216, Santa Cruz Biotechnology), mouse anti-ZO-1 (1:100; 1A12, Molecular Probes, Life Technologies) and mouse anti-Pcna (1:200; PC10, DAKO); secondary antibodies were AlexaFluor 488 or AlexaFluor 568 goat anti-mouse or goat anti-rabbit conjugates (1:200; Molecular Probes). Sections were mounted in Prolong Gold Antifade Reagent including DAPI (Invitrogen) and imaged with a Zeiss AxioImager M2 microscope equipped with ApoTome.

TUNEL labelling was performed using the Deadend Fluorometric TUNEL system (Promega) according to manufacturer's instructions. Sections were washed in PBS, counterstained with DAPI (Sigma) and mounted with Vectashield hard-set mounting medium (Vector Laboratories).

Bioinformatic analyses

All homology searches and gene annotations were carried out using the Blast2GO functional analysis suite (http://www.blast2go.com/b2ghome; B2G) (Conesa et al., 2005). An InterPro scan was performed to find functional motifs and related GO terms using the specific tool implemented in the Blast2GO software (with the default parameters). We used Fisher's exact test for the statistical analysis of GO term frequency differences between two sets of sequences identified with Enrichment Analysis tools. We used a gene list expressed in whole zebrafish CNS (data mined in ZFIN by Yan Jaszczyszyn, personal communication), together with the Ivanova hematopoiesis mature cells list of genes upregulated in mature blood

cells from adult bone marrow and fetal liver, as backgrounds for enrichment analysis. These lists are available in MSigDB v3.0 (http://www.broadinstitute.org/gsea/msigdb/index.jsp).

Ingenuity pathway analysis software (Ingenuity Systems) was used to generate networks based on their connectivity in the bibliography and in microarray experiments.

Author contributions
G.R. carried out live imaging and image analysis with the help of N.P. and T.S. who conceived Mov-IT software, and assembled the figures. J.J., A.B., A.H., E.M., F.B. and F.J. performed molecular biology and histology experiments. J.-M.H. performed electron microscopy experiments. S.D. generated the zebrafish fluorescent transgenic lines. P.H. performed the Nomarski movie. J.J. and J.-S.J. performed the datamining and gene network analysis. G.R., J.J., A.B., A.H., E.M., F.J. and J.-S.J. analysed the data and assembled the manuscript. F.J., J.-S.J. and N.P. conceived the study. G.R., F.J. and J.-S.J. wrote the manuscript with contributions from J.J., A.B., A.H., E.M., J.-M.H., F.B. and N.P.

Supplementary material
Supplementary material available online at
http://dev.biologists.org/lookup/suppl/doi:10.1242/dev.099010/-/DC1

References
Allende, M. L., Amsterdam, A., Becker, T., Kawakami, K., Gaiano, N. and Hopkins, N. (1996). Insertional mutagenesis in zebrafish identifies two novel genes, pescadillo and dead eye, essential for embryonic development. Genes Dev. 10, 3141-3155.

Alunni, A., Hermel, J. M., Heuzé, A., Bourrat, F., Jamen, F. and Joly, J. S. (2010). Evidence for neural stem cells in the medaka optic tectum proliferation zones. Dev. Neurobiol. 70, 693-713.

Amsterdam, A., Burgess, S., Golling, G., Chen, W., Sun, Z., Townsend, K., Farrington, S., Haldi, M. and Hopkins, N. (1999). A large-scale insertional mutagenesis screen in zebrafish. Genes Dev. 13, 2713-2724.

Anderson, C. M. and Parkinson, F. E. (1997). Potential signalling roles for UTP and UDP: sources, regulation and release of uracil nucleotides. Trends Pharmacol. Sci. 18, 387-392.

Arendt, D. (2005). Genes and homology in nervous system evolution: comparing gene functions, expression patterns, and cell type molecular fingerprints. Theory Biosci. 124, 185-197.

Baye, L. M. and Link, B. A. (2007). Interkinetic nuclear migration and the selection of neurogenic cell divisions during vertebrate retinogenesis. J. Neurosci. 27, 10143-10152.

Bradford, Y., Conlin, T., Dunn, N., Fashena, D., Frazer, K., Howe, D. G., Knight, J., Mani, P., Martin, R., Moxon, S. A. et al. (2011). ZFIN: enhancements and updates to the Zebrafish Model Organism Database. Nucleic Acids Res. 39, D822-D829.

Brombin, A., Grossier, J. P., Heuzé, A., Radev, Z., Bourrat, F., Joly, J. S. and Jamen, F. (2011). Genome-wide analysis of the POU genes in medaka, focusing on expression in the optic tectum. Dev. Dyn. 240, 2354-2363.

Bugner, V., Tecza, A., Gessert, S. and Kühl, M. (2011). Peter Pan functions independently of its role in ribosome biogenesis during early eye and craniofacial cartilage development in Xenopus laevis. Development 138, 2369-2378.

Development

Candal, E., Thermes, V., Joly, J. S. and Bourrat, F. (2004). Medaka as a model system for the characterisation of cell cycle regulators: a functional analysis of Ol-Gadd45gamma during early embryogenesis. *Mech. Dev.* **121**, 945-958.

Candal, E., Alunni, A., Thermes, V., Jamen, F., Joly, J. S. and Bourrat, F. (2007). Ol-insm1b, a SNAG family transcription factor involved in cell cycle arrest during medaka development. *Dev. Biol.* **309**, 1-17.

Cerveny, K. L., Varga, M. and Wilson, S. W. (2012). Continued growth and circuit building in the anamniote visual system. *Dev. Neurobiol.* **72**, 328-345.

Chapouton, P., Adolf, B., Leucht, C., Tannhäuser, B., Ryu, S., Driever, W. and Bally-Cuif, L. (2006). her5 expression reveals a pool of neural stem cells in the adult zebrafish midbrain. *Development* **133**, 4293-4303.

Chojnacki, A. K., Mak, G. K. and Weiss, S. (2009). Identity crisis for adult periventricular neural stem cells: subventricular zone astrocytes, ependymal cells or both? *Nat. Rev. Neurosci.* **10**, 153-163.

Conesa, A., Götz, S., García-Gómez, J. M., Terol, J., Talón, M. and Robles, M. (2005). Blast2GO: a universal tool for annotation, visualization and analysis in functional genomics research. *Bioinformatics* **21**, 3674-3676.

Devès, M. and Bourrat, F. (2012). Transcriptional mechanisms of developmental cell cycle arrest: problems and models. *Semin. Cell Dev. Biol.* **23**, 290-297.

Efroni, S., Duttagupta, R., Cheng, J., Dehghani, H., Hoeppner, D. J., Dash, C., Bazett-Jones, D. P., Le Grice, S., McKay, R. D., Buetow, K. H. et al. (2008). Global transcription in pluripotent embryonic stem cells. *Cell Stem Cell* **2**, 437-447.

England, S. J., Blanchard, G. B., Mahadevan, L. and Adams, R. J. (2006). A dynamic fate map of the forebrain shows how vertebrate eyes form and explains two causes of cyclopia. *Development* **133**, 4613-4617.

Fichelson, P., Moch, C., Ivanovitch, K., Martin, C., Sidor, C. M., Lepesant, J. A., Bellaiche, Y. and Huynh, J. R. (2009). Live-imaging of single stem cells within their niche reveals that a U3snoRNP component segregates asymmetrically and is required for self-renewal in Drosophila. *Nat. Cell Biol.* **11**, 685-693.

Fuchs, E., Tumbar, T. and Guasch, G. (2004). Socializing with the neighbors: stem cells and their niche. *Cell* **116**, 769-778.

Geldmacher-Voss, B., Reugels, A. M., Pauls, S. and Campos-Ortega, J. A. (2003). A 90-degree rotation of the mitotic spindle changes the orientation of mitoses of zebrafish neuroepithelial cells. *Development* **130**, 3767-3780.

Götz, M. and Huttner, W. B. (2005). The cell biology of neurogenesis. *Nat. Rev. Mol. Cell Biol.* **6**, 777-788.

Grandel, H. and Brand, M. (2013). Comparative aspects of adult neural stem cell activity in vertebrates. *Dev. Genes Evol.* **223**, 131-147.

Grandel, H., Kaslin, J., Ganz, J., Wenzel, I. and Brand, M. (2006). Neural stem cells and neurogenesis in the adult zebrafish brain: origin, proliferation dynamics, migration and cell fate. *Dev. Biol.* **295**, 263-277.

Greiling, T. M., Aose, M. and Clark, J. I. (2010). Cell fate and differentiation of the developing ocular lens. *Invest. Ophthalmol. Vis. Sci.* **51**, 1540-1546.

Herbomel, P. (1999). Spinning nuclei in the brain of the zebrafish embryo. *Curr. Biol.* **9**, R627-R628.

Hölzel, M., Rohrmoser, M., Schlee, M., Grimm, T., Harasim, T., Malamoussi, A., Gruber-Eber, A., Kremmer, E., Hiddemann, W., Bornkamm, G. W. et al. (2005). Mammalian WDR12 is a novel member of the Pes1-Bop1 complex and is required for ribosome biogenesis and cell proliferation. *J. Cell Biol.* **170**, 367-378.

Hsieh, J. (2012). Orchestrating transcriptional control of adult neurogenesis. *Genes Dev.* **26**, 1010-1021.

Ito, Y., Tanaka, H., Okamoto, H. and Ohshima, T. (2010). Characterization of neural stem cells and their progeny in the adult zebrafish optic tectum. *Dev. Biol.* **342**, 26-38.

Kimmel, C. B., Ballard, W. W., Kimmel, S. R., Ullmann, B. and Schilling, T. F. (1995). Stages of embryonic development of the zebrafish. *Dev. Dyn.* **203**, 253-310.

Kizil, C., Kaslin, J., Kroehne, V. and Brand, M. (2011). Adult neurogenesis and brain regeneration in zebrafish. *Dev. Neurobiol.* **72**, 429-461.

Komili, S., Farny, N. G., Roth, F. P. and Silver, P. A. (2007). Functional specificity among ribosomal proteins regulates gene expression. *Cell* **131**, 557-571.

Kondrashov, N., Pusic, A., Stumpf, C. R., Shimizu, K., Hsieh, A. C., Xue, S., Ishijima, J., Shiroishi, T. and Barna, M. (2011). Ribosome-mediated specificity in Hox mRNA translation and vertebrate tissue patterning. *Cell* **145**, 383-397.

Koudijs, M. J., den Broeder, M. J., Keijser, A., Wienholds, E., Houwing, S., van Rooijen, E. M., Geisler, R. and van Eeden, F. J. (2005). The zebrafish mutants dre, uki, and lep encode negative regulators of the hedgehog signaling pathway. *PLoS Genet.* **1**, e19.

Kriegstein, A. and Alvarez-Buylla, A. (2009). The glial nature of embryonic and adult neural stem cells. *Annu. Rev. Neurosci.* **32**, 149-184.

Kwan, K. M., Otsuna, H., Kidokoro, H., Carney, K. R., Saijoh, Y. and Chien, C. B. (2012). A complex choreography of cell movements shapes the vertebrate eye. *Development* **139**, 359-372.

Law, J. A. and Jacobsen, S. E. (2010). Establishing, maintaining and modifying DNA methylation patterns in plants and animals. *Nat. Rev. Genet.* **11**, 204-220.

Le Boutellier M., Souilhol C., Beck-Cormier S., Stedman A., Burlen-Defranoux O., Vandormael-Pournin S., Bernex F., Cumano A. and Cohen-Tannoudji M. (2013). Notchless-dependent ribosome synthesis is required for the maintenance of adult hematopietic stem cells. *J. Exp. Med.* **210**, 2351-2369.

Link, B. A., Kainz, P. M., Ryou, T. and Dowling, J. E. (2001). The perplexed and confused mutations affect distinct stages during the transition from proliferating to post-mitotic cells within the zebrafish retina. *Dev. Biol.* **236**, 436-453.

Liu, Y. C., Li, F., Handler, J., Huang, C. R., Xiang, Y., Neretti, N., Sedivy, J. M., Zeller, K. I. and Dang, C. V. (2008). Global regulation of nucleotide biosynthetic genes by c-Myc. *PLoS ONE* **3**, e2722.

Locker, M., Agathocleous, M., Amato, M. A., Parain, K., Harris, W. A. and Perron, M. (2006). Hedgehog signaling and the retina: insights into the mechanisms controlling the proliferative properties of neural precursors. *Genes Dev.* **20**, 3036-3048.

Mathis, L. and Nicolas, J. F. (2006). Clonal origin of the mammalian forebrain from widespread oriented mixing of early regionalized neuroepithelium precursors. *Dev. Biol.* **293**, 53-63.

Mishra, S., Murphy, L. C. and Murphy, L. J. (2006). The Prohibitins: emerging roles in diverse functions. *J. Cell. Mol. Med.* **10**, 353-363.

Müller, F. J., Laurent, L. C., Kostka, D., Ulitsky, I., Williams, R., Lu, C., Park, I. H., Rao, M. S., Shamir, R., Schwartz, P. H. et al. (2008). Regulatory networks define phenotypic classes of human stem cell lines. *Nature* **455**, 401-405.

Neumüller, R. A., Richter, C., Fischer, A., Novatchkova, M., Neumüller, K. G. and Knoblich, J. A. (2011). Genome-wide analysis of self-renewal in Drosophila neural stem cells by transgenic RNAi. *Cell Stem Cell* **8**, 580-593.

Olivier, N., Luengo-Oroz, M. A., Duloquin, L., Faure, E., Savy, T., Veilleux, I., Solinas, X., Débarre, D., Bourgine, P., Santos, A. et al. (2010). Cell lineage reconstruction of early zebrafish embryos using label-free nonlinear microscopy. *Science* **329**, 967-971.

Palmgren, A. (1921). Embryological and morphological studies on the mid-brain and cerebellum of vertebrates. *Acta Zoologica* **2**, 1-94.

Parain, K., Mazurier, N., Bronchain, O., Borday, C., Cabochette, P., Chesneau, A., Colozza, G., El Yakoubi, W., Hamdache, J., Locker, M. et al. (2011). A large scale screen for neural stem cell markers in Xenopus retina. *Dev. Neurobiol.* **72**, 491-506.

Perrera, C., Colombo, R., Valsasina, B., Carpinelli, P., Troiani, S., Modugno, M., Gianellini, L., Cappella, P., Isacchi, A., Moll, J. et al. (2010). Identification of Myb-binding protein 1A (MYBBP1A) as a novel substrate for aurora B kinase. *J. Biol. Chem.* **285**, 11775-11785.

Peyre, E., Jaouen, F., Saadaoui, M., Haren, L., Merdes, A., Durbec, P. and Morin, X. (2011). A lateral belt of cortical LGN and NuMA guides mitotic spindle movements and planar division in neuroepithelial cells. *J. Cell Biol.* **193**, 141-154.

Ramialison, M., Reinhardt, R., Henrich, T., Wittbrodt, B., Kellner, T., Lowy, C. M. and Wittbrodt, J. (2012). Cis-regulatory properties of medaka synexpression groups. *Development* **139**, 917-928.

Rieger, S., Wang, F. and Sagasti, A. (2011). Time-lapse imaging of neural development: zebrafish lead the way into the fourth dimension. *Genesis* **49**, 534-545.

Rinkwitz, S., Mourrain, P. and Becker, T. S. (2011). Zebrafish: an integrative system for neurogenomics and neurosciences. *Prog. Neurobiol.* **93**, 231-243.

Rothenaigner, I., Krecsmarik, M., Hayes, J. A., Bahn, B., Lepier, A., Fortin, G., Götz, M., Jagasia, R. and Bally-Cuif, L. (2011). Clonal analysis by distinct viral vectors identifies bona fide neural stem cells in the adult zebrafish telencephalon and characterizes their division properties and fate. *Development* **138**, 1459-1469.

Ruggero, D. and Pandolfi, P. P. (2003). Does the ribosome translate cancer? *Nat. Rev. Cancer* **3**, 179-192.

Schmidt, R., Strähle, U. and Scholpp, S. (2013). Neurogenesis in zebrafish - from embryo to adult. *Neural Dev.* **8**, 3.

Sheng, J., Yang, S., Xu, L., Wu, C., Wu, X., Li, A., Yu, Y., Ni, H., Fukuda, M. and Zhou, J. (2004). Bystin as a novel marker for reactive astrocytes in the adult rat brain following injury. *Eur. J. Neurosci.* **20**, 873-884.

Sigoillot, F. D., Evans, D. R. and Guy, H. I. (2002). Growth-dependent regulation of mammalian pyrimidine biosynthesis by the protein kinase A and MAPK signaling cascades. *J. Biol. Chem.* **277**, 15745-15751.

Solnica-Krezel, L., Schier, A. F. and Driever, W. (1994). Efficient recovery of ENU-induced mutations from the zebrafish germline. *Genetics* **136**, 1401-1420.

Steinmetz, P. R., Kostyuchenko, R. P., Fischer, A. and Arendt, D. (2011). The segmental pattern of otx, gbx, and Hox genes in the annelid Platynereis dumerilii. *Evol. Dev.* **13**, 72-79.

Subramanian, A., Tamayo, P., Mootha, V. K., Mukherjee, S., Ebert, B. L., Gillette, M. A., Paulovich, A., Pomeroy, S. L., Golub, T. R., Lander, E. S. et al. (2005). Gene set enrichment analysis: a knowledge-based approach for interpreting genome-wide expression profiles. *Proc. Natl. Acad. Sci. USA* **102**, 15545-15550.

Tsuchiya, M., Katagiri, N., Kuroda, T., Kishimoto, H., Nishimura, K., Kumazawa, T., Iwasaki, N., Kimura, K. and Yanagisawa, J. (2011). Critical role of the nucleolus in activation of the p53-dependent postmitotic checkpoint. *Biochem. Biophys. Res. Commun.* **407**, 378-382.

Willer, G. B., Lee, V. M., Gregg, R. G. and Link, B. A. (2005). Analysis of the Zebrafish perplexed mutation reveals tissue-specific roles for de novo pyrimidine synthesis during development. *Genetics* **170**, 1827-1837.

Xu, Q., Holder, N., Patient, R. and Wilson, S. W. (1994). Spatially regulated expression of three receptor tyrosine kinase genes during gastrulation in the zebrafish. *Development* **120**, 287-299.

Xue, X. Y. and Harris, W. A. (2011). Using myc genes to search for stem cells in the ciliary margin of the Xenopus retina. *Dev. Neurobiol.* **72**, 475-490.

Zhang, Y., Duc, A. C., Rao, S., Sun, X. L., Bilbee, A. N., Rhodes, M., Li, Q., Kappes, D. J., Rhodes, J. and Wiest, D. L. (2013). Control of hematopoietic stem cell emergence by antagonistic functions of ribosomal protein paralogs. *Dev. Cell* **24**, 411-425.

Zhao, C., Deng, W. and Gage, F. H. (2008). Mechanisms and functional implications of adult neurogenesis. *Cell* **132**, 645-660.

Zupanc, G. K. (2009). Towards brain repair: Insights from teleost fish. *Semin. Cell Dev. Biol.* **20**, 683-690.

Zupanc, G. K. and Sîrbulescu, R. F. (2011). Adult neurogenesis and neuronal regeneration in the central nervous system of teleost fish. *Eur. J. Neurosci.* **34**, 917-929.